Universiteit
Leiden
The Netherlands

Identification of therapeutic targets in coronary artery disease: from patient to mice and back

Kraaijeveld, A.O.

Citation
Kraaijeveld, A. O. (2009, October 1). *Identification of therapeutic targets in coronary artery disease: from patient to mice and back*. Retrieved from https://hdl.handle.net/1887/14029

Version:	Corrected Publisher's Version
License:	Licence agreement concerning inclusion of doctoral thesis in the Institutional Repository of the University of Leiden
Downloaded from:	https://hdl.handle.net/1887/14029

Note: To cite this publication please use the final published version (if applicable).

CHAPTER 8

Age dependent impairment of adaptive vascular remodeling in LDLr-/- mice suggests an association of Quaking in atherosclerosis

Adriaan O. Kraaijeveld
Ramon de Nooijer
Peter-Bram C. 't Hoen
W. Bob Meijboom
Christian A. van der Lans
Arjan H. Schoneveld
Dominique P. de Kleijn
Theo J.C. van Berkel
J. Wouter Jukema
Erik A.L. Biessen

Manuscript submitted

ABSTRACT

Objective: Aging is regarded as a major risk factor for cardiovascular diseases. In this study we have assessed whether age per se affects the atherogenic response in LDLr-/- mice.

Methods and results: Atherosclerotic lesions were elicited in carotid arteries of young (12 weeks) and aged (52 weeks) LDLr-/- mice by perivascular collar placement through six weeks of Western-type diet. Cholesterol levels upon high fat feeding were consistently higher in young vs. aged mice (baseline sample 1690 vs. 1294 mg/dl; $P<0.001$). Six weeks after surgery, carotid plaque (40,500 vs. 14,800 μm^2, $P<0.04$) and media areas (52,300 vs. 33,600 μm^2, $P<0.02$) were larger in young mice. Paradoxically however, due to the effective compensatory remodeling (+63% vs. +30% in aged mice), their lumen size was increased (86,500 vs. 65,100 μm^2, $P<0.04$). Similar to carotid plaques, aortic sinus plaques in young mice were larger ($7,38x10^5$ vs. $5,06x10^5$ μm^2, $P<0.03$) as well. No fundamental differences were observed in plaque composition or in plaque stability. Microarray analysis of atherosclerotic carotid arteries from both groups identified 41 differentially regulated genes, at which genes of the vasculogenesis pathway were particularly overrepresented. This was corroborated immunohistochemically, showing that Quaking, one of the key genes in vasculogenesis, was abundantly expressed in mouse and human atheromata.

Conclusions: Age is accompanied by an impaired capacity to adapt to changes in diet cholesterol loads, and by a decreased atherogenenic and diminished outward remodeling response in LDLr-/- mice. Aging induces differential expression of 41 genes in the carotid artery, of which Qk seems of particular interest in relation to its potential regulatory role in vascular remodeling.

INTRODUCTION

In 1963 McGill et al. postulated a relationship between aging and increased atherosclerotic burden, and today aging is considered one of the major independent atherosclerotic risk factors [1]. Vascular aging is a complex process which is not only the consequence of prolonged exposure to various pro-atherogenic risk factors but also of intrinsic factors in the aging process itself which enhance the susceptibility towards atherosclerosis [2].

Various components of the vascular wall progressively lose part of their functional capacity during aging. For instance the endothelium will express more adhesion molecules facilitating monocyte influx into the intima and will produce less nitric oxide, thereby decreasing vasodilatory capacity and increasing endothelial permeability, aggravating clinical outcome [3, 4,5]. At the same time, the vessel wall gradually stiffens due to an increase in collagen content and collagen cross-linking, as well as by a decrease in elastin, which gets calcified and fragmentised [6]. However, contradictory reports exist on the effect of aging on vascular smooth muscle cells (VSMCs). VSMCs derived from old rats show, in comparison with VSMCs derived from young rats, an age-related increase in proliferative capacity, whereas humane cultured VSMCs obtained from young persons clearly show an increased proliferative capacity as compared with cells from aged persons [7, 8,9, 10]. Taken together, increased vascular stiffening and decreased VSMC proliferation may hamper the vascular outward remodeling response [11].

Since the direct effect of aging on atherosclerotic lesion initiation and progression is difficult to address in humans, an animal model is imperative. However, most animal studies which explored the influence of aging on atherosclerosis in fact investigated temporal lesion progression rather than intrinsic atherogenecity applying a continuous period of high fat feeding throughout the study, thus mimicking the human situation. So far, only few publications investigated age related differences in intrinsic atherogenicity after an identical period of high fat feeding. Cortes showed that young rabbits exhibited an enhanced atherogenic response compared with old rabbits after exposure to a similar lipid load, while opposite findings were reported by Orlandi in a similar set-up in mice [12,13]. Our study is designed to 1) map whether plaque growth, composition and stability are altered with age at various locations within the arterial tree in Western type diet fed LDLr-/- mice. Furthermore, 2) we test the hypothesis that aged mice display a reduced capacity for atherosclerosis induced adaptive outward remodeling. Finally, as the genetic determinants of vascular aging are largely unknown, 3) we map differentially regulated genes and genetic pathways in young versus aged mice which can be linked with age dependent differences in atherogenesis or vascular remodeling.

METHODS

Animals

Female LDLr -/- mice, aged 12 weeks (n=16) and 52 weeks (n=14), were obtained from our own breeding stock. Mice were placed on a western-type diet containing 0.25% cholesterol and 15% cocoa butter (Special Diets Services, Witham, Essex, UK). Diet and water were provided ad libitum. All animal work was approved by the regulatory authority of Leiden University and performed in compliance with the Dutch government guidelines.

Collar Placement

After 2 weeks of western-type diet, carotid atherosclerotic lesions were induced by perivascular bilateral collar placement as previously described [14]. Mice were anesthetized with a subcutaneous injection of ketamine (60 mg/kg; Eurovet, Bladel, the Netherlands), fentanyl citrate and fluanisone (1,26 mg/kg and 2 mg/kg, respectively; Jansen Animal Health, Beerse, Belgium). The mice were sacrificed 6 weeks after collar placement.

Plasma and Hepatic Analysis

Every two weeks, blood samples were taken via tail vein incision and plasma cholesterol levels were monitored colorimetrically using enzymatic procedures (Roche Diagnostics, Mannheim, Germany). Lipoprotein fractions were determined using a Superose 6 column (Smart system, Pharmacia, Uppsala, Sweden) at collar placement. Insulin levels were measured using an ELISA assay (Mercodia, Sweden), glucose levels were colorimetrically determined as described by Reljic [15]. Hepatic lipid concentrations were determined using the method of Bligh and Dyer [16].

Tissue Harvesting and Histological Analysis

Mice were sacrificed six weeks after collar placement. Before harvesting, the arterial bed was flushed for ten minutes with phosphate buffered saline (PBS) and formaldehyde. The right carotid artery and liver were frozen in liquid nitrogen and stored at -80ºC until further analysis. Transverse, serial cryosections were prepared from OCT-compound (Sakura Finetek) embedded left carotid and brachiocephalic arteries (5µm thick) as well as hearts (10µm thick) and routinely stained with hematoxylin (Sigma Diagnostics), eosin (Merck Diagnostica) and accustain trichrome (Sigma Diagnostics). Collagen staining was performed by a 90 minute incubation of cryosections in 0.1% Picro Sirius Red (Direct red 80, Sigma Diagnostics) in saturated picric acid and subsequent lysing in 0.01M HCL and distilled water. Lipid fractions were stained for ten minutes in 0.5% Oil-red-O (Sigma Diagnostics). Corresponding sections were stained immunohistochemically with antibodies directed against α-actin for smooth muscle cells (monoclonal rat IgG, clone 1A4, dilution 1:250; Sigma Diagnostics), metallophilic macrophages (monoclonal rat IgG2a, clone MOMA2, dilution 1:50; Sigma Diagnostics). Intimal apoptosis was visualized using the TUNEL staining method (Roche Diagnostics).

Morphometry

All plaque and vessel areas were assessed in hematoxylin and eosin stained cryosections and analyses was digitally performed as previously described [14]. As a reference measure of non-remodeled carotid arteries we have determined vessel areas derived from the EEL circumference at the plaque free segment caudally to the site of the collar induced plaques (figure 3A). Luminal stenosis (%) was defined by the true luminal area divided by the internal elastic laminar area x 100.

Macrophage-, smooth muscle cell- and collagen-positive areas were determined by computer-assisted color-gated measurement using LeicaQwin software (Leica Imaging Systems, Cambridge, UK), and related to the total plaque area. TUNEL positive cells were counted and related to the total number of plaque cells. The extent of internal elastic lamina ruptures was scored using consecutive HE sections by fluorescent microscopy to visualize elastin.

Gene expression analysis

Gene expression analysis was performed by real time-PCR on a ABI Prism 7700 Sequence detector (Applied Biosystems, Foster city, CA) using the SYBR Green (Eurogentec) technology and with primer pairs given in supplemental table 1. The mean threshold cycle numbers (Ct) of Hypoxanthine guanine phosphoribosyl transferase (HPRT) and 18S were averaged and used as housekeeping genes. The relative gene expression was calculated by subtracting the Ct of the target gene from the average household Ct and rising to the power of this difference.

Immunohistochemistry

Qk protein expression was assessed both in mouse carotid arteries and heart sections as well as in human atherosclerotic plaques derived from coronary arteries (kindly provided by dr. J. von der Thüsen, Department of Pathology, Leiden University Medical Center) with a goat-anti-rabbit Qk antibody (1:500, Bethyl laboratories, Montgomery, TX) and hematoxylin counterstaining. Isotype control staining was performed with a rabbit IgG antibody at identical concentration (Santa Cruz Biotechnology, Santa Cruz, CA). For optimal visualization, the staining signal was amplified by the CSA system with diaminobenzidine tetrahydrochloride (DAB) as substrate (Dako, the Netherland

Carotid Artery Microarray Gene Profiling

Snap frozen carotid arteries were pooled in four subgroups of three samples per age group in order to yield a sufficient amount of RNA, and samples were homogenized in Guanidium thiocyanate-phenol reagent. After RNA extraction, RNA was further purified using an RNeasy mini column (Qiagen, Venlo, the Netherlands). On average 130 to 500 ng of total RNA was amplified (1x) according to the Eberwine procedure by the Ambion amplifying kit (Ambion, Austin, TX) [17]. Total RNA quality was assessed by the lab-on-chip Agilent 2100 Bioanalyzer (Agilent, Palo Alto, CA). Aminoallyl UTPs (A5660, Sigma Diagnostics) were incorporated during in vitro transcription and 3 micrograms of aminoallyl-modified nucleotides were coupled with

monoreactive Cy3 and Cy5 dyes (Amersham, Piscataway, NJ). Subsequently, oligonucleotide micro array slides (Sigma-Compugen mouse library version I, consisting of 21,668 65mer oligonucleotides, printed at the Leiden Genome Technology Center, the Netherlands) were hybridized in a GeneTAC hybridization station (Genomic Solutions, Ann Arbor, MI). Individual pools of young and old mice were co-hybridized on the same slides. Each pool was hybridized once in Cy3 and once in Cy5 (dye-swap design), resulting in a total of 8 slides. Slides were scanned in an Agilent G2565BA microarray scanner. Feature and background intensities values were evaluated with GenePix v5.0 (Molecular Devices, Sunnyvale, CA). After normalization using Rosetta Resolver's default error model for GenePix files, a one-group student's t-test was applied to test if the ratio between old and young mice was significantly different from zero. P-values were corrected for multiple testing using Benjamini and Hochberg false discovery rate [18]. Gene Ontology Tree Machine (GOTM) software, a web-based tool (see http://bioinfo.vanderbilt.edu/gotm/) for analysis of high-throughput data, was used to transfer the expression profile results into functional categories [19]. To verify differences in gene-expression, primers were designed using PrimerExpress 1.5 (Applied Biosystems, Foster City, CA) and quantitative real time PCR analysis was performed as described in the data supplement.

Age related Quaking Expression analysis

Aortic cDNA from C57Bl/6J (n=6 per group) and ApoE-/- (n=10 per group) mice, sacrificed at 5, 10, 15, 25 and 40 weeks of age fed normal chow diet was used for verification of aging induced differences in Quaking (Qk) expression levels [20]. Real time PCR was performed on an I-cycler apparatus using the SYBR Green technology (Biorad, Hercules, CA) with Qk-F (TTCACTTCTTCAACCGCTCTC) and Qk-R (CAAAGGCTCAATGAGGGATAA) as primers. Relative expression levels were calculated with 18S as housekeeping gene.

Statistics

Differences in plaque size, other plaque parameters and gene expression levels were statistically analyzed by Student's t-test or the non parametric Mann-Whitney U-test when appropriate. Plaque morphology data were analyzed by Fisher's exact test and correlations were examined by Pearson correlation analysis. Micro-array data were analyzed by Student's t-test and subsequently corrected for multiple testing according to Benjamini and Hochberg. Age dependent Quaking expression was analyzed by oneway ANOVA and Tuckey's multiple comparison tests. All data are given as mean ± S.E.M. and P-values <0.05 were considered significant. All statistical analyses were performed by GraphPad Prism software version 4.3 (Graphpad software, San Diego, CA), except for the micro-array experiment, where Rosetta Resolver software (Rosetta Biosoftware, Seattle, WA) was applied.

RESULTS

At the start of the study, the young mice weighed significantly less than the aged mice. During the course of the study the young mice gained weight and the initial difference faded out (start: 19 ± 4.3 vs. 25 ± 2.8 g, P<0.01; sacrifice: 24 ± 3.6 vs. 26 ± 2.3 g, P=0.1)(figure 1A).

Figure 1.

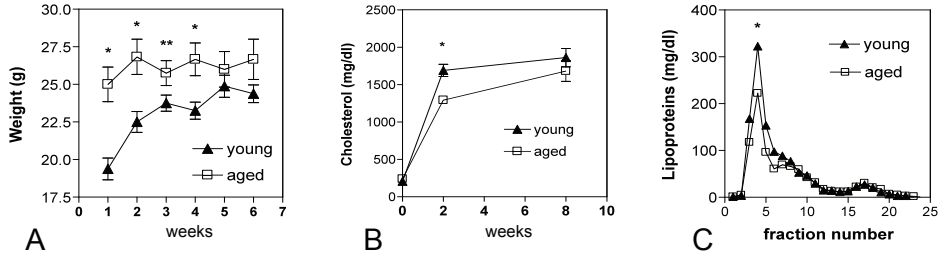

Young and aged mice differed significantly in body weight at the start of the experiment. During the course of the experiment, young mice gained weight and finally there were no significant differences between groups (A). A diet induced rise in serum cholesterol level is seen to be delayed in aged vs. young mice after starting the Western type diet; at the time of sacrifice no differences are observed (B). Lipoprotein analysis performed at collar placement show a small but significant difference in the VLDL fraction of young vs. aged mice (C). Values are mean ± SEM. * P<0.01, ** P<0.05

Initial increased cholesterol levels in young mice

While cholesterol levels of young and aged mice were on chow were essentially similar, two weeks after initiation of the high fat diet at collar placement, the young mice displayed marked higher total cholesterol levels (pre-diet: 206 ± 38 vs. 239 ± 16 mg/dl, P=0.14; diet: 1690 ± 331 vs. 1294 ± 325 mg/dl, P<0.01)(figure 1B). Analysis of the lipoprotein profile at collar placement revealed a significant difference only in the very low density lipoprotein fraction (153 ± 23 vs. 96 ± 13 mg/dl, P=0.01), no differences were seen in LDL and HDL levels (figure 1C). At the end of the experiment after eight weeks of high fat feeding, the initial difference in serum cholesterol levels between young and aged mice was not seen. Additional analysis at sacrifice for serum

Figure 2.

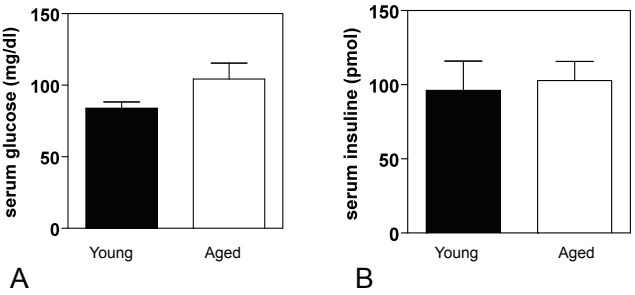

Serum glucose levels are increased in aged mice (P=0.09), however no overt differences are seen in serum insulin levels between groups (A,B). Values are mean ± SEM.

insulin levels also did not reveal any differences (96 ± 71 vs. 103 ± 40 pmol, P=0.73), although serum glucose levels tended to be higher in the aged mice at sacrifice (84 ± 17 vs. 104 ± 37 mg/dl, P=0.09)(figure 2A,B). Hepatic lipid analyses revealed no obvious differences between groups either (data not shown).

Increased atherogenesis in young mice

Plaque size analysis at the right carotid artery (figure 3A, site A) revealed a remarkably larger lesion burden in young mice ($40x10^3 \pm 35x10^3$ vs. $17x10^3 \pm 16x10^3$ μm^2, P<0.05), accompanied by more extensive media expansion ($46x10^3 \pm 17x10^3$ vs. $29x10^3 \pm 9.7x10^3 \mu m^2$; P=0.01). Although young mice tended to experience more luminal stenosis (45 ± 34 vs. 24 ± 22%, P=0.09), lumen areas however did not differ between groups ($44x10^3 \pm 28x10^3$vs. $47x10^3 \pm 22x10^3$ μm^2, P=0.78) (figure 3A-C). In keeping, total vessel area (TVA) as measured by the area within the circumference of the external elastic lamina was markedly increased in the young mice ($132x10^3 \pm 28 x10^3$ vs. $94x10^3 \pm 32x10^3$ μm^2, P<0.01)(figure 3B). Interestingly, correlation analysis revealed a highly significant correlation between plaque size and TVA in young mice (r=0.80, P<0.001), whereas in aged mice, this correlation could not be detected (r=0.35, P=0.32). The mean TVA of the plaque free reference site further upstream of the carotid artery plaque did not differ between groups ($80x10^3 \pm 21 x10^3$ vs. $72x10^3 \pm 28 x10^3$ μm^2, P=0.53, figure 3B, site B). Young mice therefore showed a 63% increase in TVA compared with 30% in aged mice, which could point towards an age-related impaired remodeling capacity in response to collar induced atherogenesis in aged mice.

At the level of the brachiocephalic artery, plaque size in young mice tended to be increased ($59x10^3 \pm 43 x10^3$ vs. $38x10^3 \pm 31 x10^3$ μm^2, P=0.20). In concordance with the carotid plaque data, plaque size at the level of the aortic root was larger in young mice ($7.35x10^5 \pm 2.1 x10^5$ vs.

Figure 3.

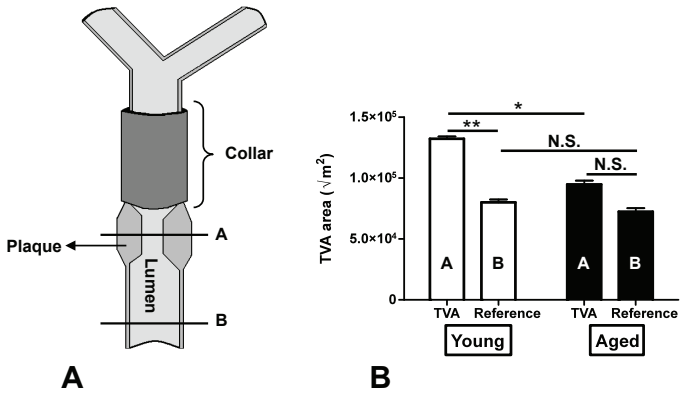

Illustration of the collar induced atherosclerosis mouse model. Atherosclerosis develops proximal of the collar orifice at site A with concomitant outward vascular remodeling. Transverse sections at site B are used to determine reference total vessel area (TVA) in each carotid artery (Figure 1A.). TVA differs between young and aged mice at site A, whereas reference TVA at site B is equal (Figure 1B.). Furthermore, TVA significantly differs between sites A and B in young mice, but not in aged mice. Values are mean ± SEM. * P < 0.01, ** P < 0.001, N.S. = non-significant

$5.06x10^5 \pm 2.1\ x10^5 \mu m^2$, P<0.01) (figure 4I). The differences in lesion size at these locations indicate that the increased atherogenic response in young mice is a generalized phenomenon in various vascular beds and therefore not merely due to collar placement in the carotid artery. Of note, lesions sizes were not biased by differences in cholesterol levels, as there was no correlation between these two parameters both for aortic root and carotid sections (data not shown).

No difference in plaque composition and stability

In line with these observations, there were no differences in TUNEL positive cells, internal elastic lamina ruptures, macrophage and collagen content of plaques. However, we did observe a higher non-significant (P=0.16) smooth muscle cell presence in the aged group, as judged from the increased α-actin staining (figure 4D-H). Therefore, aging per se does not seem to influence the morphometric stability parameters of carotid artery plaques. In the aortic root, we did observe an increased collagen content in the young mice (8.1 ± 4.7 vs. 3.3 ± 2.1 %, P<0.01) (figure 4J).

Figure 4.

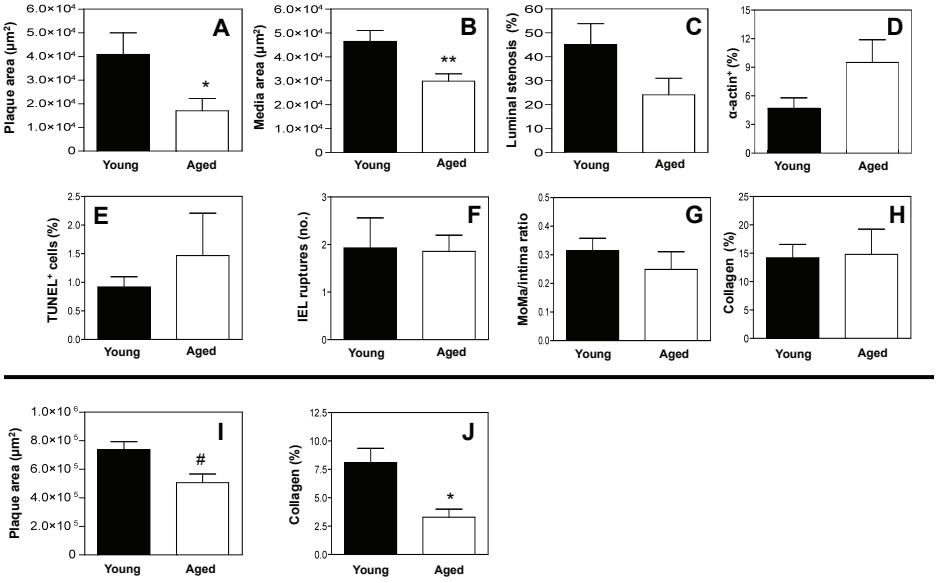

Plaque as well as media areas are significantly larger in the carotid artery of young mice after collar placement. The percentage of luminal stenosis tends to be increased in the young mice as well, although not significant (A-C). Regarding plaque stability parameters, no significant differences are observed in vascular smooth muscle cell content as assessed via α-actin SM staining (D), percentage of apoptotic cells (E), ruptures of the internal elastic lamina (F), percentage of neo-intimal monocytes (G) and collagen content (H). Plaque size is larger in young mice at the aortic root level as well (I), and we observe a decreased collagen content in aged plaques (J). Values are mean ± SEM. * P=0.05, ** P=0.01, # P<0.01, N.S. = non-significant

Microarray expression analysis

To detect age related differences in vascular wall gene expression, we performed microarray analysis on a segment of the left carotid arteries which included the vascular wall and resident atherosclerotic plaque. With a false discovery rate of 10%, 21 genes (minimal fold change -1.2, maximum -2.5) were found down-regulated in the arteries of aged compared to young mice, whereas 20 genes (minimal fold change 1.2, maximum 2.1) were found up-regulated (table 1A,B). Up- and down-regulated genes listed in table 1 were uploaded in the online GOTM program for categorization into the three main Gene Ontology (GO) sectors, i.e. biological process, molecular function and cellular function. A hypergeometric test was applied to analyze which GO categories were enriched (P-value <0.01) in the list of differentially expressed genes when compared to all genes on the array (figure 5). Aging did not cause a generalized shift in gene expression profile, but was accompanied by changes in 8 specific GO categories. "Vasculature development" and three down-stream categories were significantly enriched, containing three up-regulated genes (Nr2f2, Hey2 and Quaking)(figure 5). The "cellular physiological process" box, a very broad category, was also enriched, with 28 differentially regulated genes (12 up, 16 down). Further down-stream, only "vitamin metabolism" was enriched, as two down-regulated genes (Lcn5 and Tpk1) were observed in the aged mice. Finally, the "ubiquitin thiolesterase activity" (Usp3 and Usp4) and "intramolecular oxidoreductase activity" (Lcn5 and Gnpda2) categories, two other enriched down-stream GO categories of "molecular function", both contained one up- and one down-regulated gene. Subsequent real time-PCR verification analysis

Table 1A. Down-regulated genes in aged vs. young mouse carotid arteries.

Symbol	Accession #	P-value	Fold Change	Name
Abhd1	NM_021304	0.0	-2.2	Alfa/beta hydrolase domain containing 1
Alas2	M63244	8.21×10^{-11}	-2.1	Aminolevulinic acid synthase 2, erythroid
Apoa5	AF327059	9.81×10^{-45}	-2.3	Apolipoprotein A-V
Bckdk	NM_009739	2.76×10^{-08}	-1.3	Branched chain ketoacid dehydrogenase kinase
Cat	M29394	3.23×10^{-12}	-1.9	Catalase
Cdca5	NM_026410	4.42×10^{-17}	-1.7	Cell division cycle associated 5
Def6	AK010356	4.93×10^{-16}	-1.7	Differentially expressed in FDCP 6
Eef2	M76131	3.98×10^{-15}	-1.3	Eukaryotic translation elongation factor 2
Fabp1	NM_017399	1.47×10^{-12}	-2.5	Fatty acid binding protein 1, liver
Gtlf3b	NM_025294	7.70×10^{-22}	-1.4	Gene trap locus F3b
Lcn5	NM_007947	6.14×10^{-15}	-1.8	Lipocalin 5
Man2a2	AK006777	6.79×10^{-09}	-1.4	Mannosidase 2, α2
Mll	L17069	4.28×10^{-07}	-1.2	Myeloid/lymphoid or mixed-lineage leukemia
Spint2	AF099016	1.40×10^{-45}	-1.8	Serine protease inhibitor, Kunitz type 2
Tex261	NM_009357	5.34×10^{-09}	-1.3	Testis expressed gene 261
Tesk1	NM_011571	8.41×10^{-11}	-1.3	Testis specific protein kinase 1
Thap11	NM_021513	6.59×10^{-15}	-1.3	THAP domain containing 11
Tpk1	NM_013861	3.31×10^{-21}	-1.6	Thiamin pyrophosphokinase
Tm4sf5	BC010782	1.16×10^{-12}	-1.5	Transmembrane 4 superfamily member 5
Trim29	BC006699	3.51×10^{-10}	-1.7	Tripartite motif protein 29
Usp4	NM_011678	2.26×10^{-10}	-1.3	Ubiquitin specific protease 4 (proto-oncogene)

Table 1B. Up-regulated genes in aged vs. young mouse carotid arteries.

Symbol	Accession #	P-value	Fold Change	Name
Abi2	AK018440	1.88×10^{-9}	1.6	Abl-interactor 2
Cpeb1	NM_007755	2.06×10^{-7}	1.6	Cytoplasmic polyadenylation element binding protein 1
Gnpda2	BC004084	1.22×10^{-23}	1.6	Expressed sequence AA407526
Fmnl2	AK017338	2.09×10^{-16}	2.1	Formin-like 2
Hey2	NM_013904	4.76×10^{-8}	1.5	Hairy/enhancer-of-split related with YRPW motif 2
Hspa8	M19141	1.22×10^{-20}	1.6	Heat shock protein 8
Ik	AJ006130	3.25×10^{-15}	1.5	IK cytokine
Igh-6	M18505	1.00×10^{-16}	2.0	Immunoglobulin heavy chain 6 (heavy chain of IgM)
Max	NM_008558	2.89×10^{-8}	1.3	Max protein
Nr2f2	NM_009697	1.43×10^{-42}	2.1	Nuclear receptor subfamily 2, group F, member 2
Pdcl3	BC005601	9.12×10^{-9}	1.2	Phosducin-like 3
Polr3a	AK020383	1.57×10^{-12}	1.3	Polymerase (RNA) III (DNA directed) polypeptide A
Ppm1a	NM_008910	5.22×10^{-11}	1.4	Protein phosphatase 1A, magnesium dependent, α isoform
Qk	NM_021881	2.28×10^{-10}	1.7	Quaking
Rraga	AK004955	3.26×10^{-12}	1.4	Ras-related GTP binding A
Arhgef3	BC012262	9.84×10^{-16}	1.5	Rho guanine nucleotide exchange factor (GEF) 3
Tgfb3	NM_009368	1.08×10^{-12}	1.2	Transforming growth factor, β3
Tmeff1	AJ400622	4.85×10^{-13}	1.5	Transmembrane protein with EGF-like and two follistatin-like domains 1
Usp33	BC005506	9.38×10^{-13}	1.4	Ubiquitin specific protease 33
Wsb1	NM_019653	6.75×10^{-8}	1.3	WD repeat and SOCS box-containing 1
Z	AK009725	2.89×10^{-16}	1.3	Zinc finger protein 180

in the four pooled samples per age group, performed on a selected set of genes involved in these different categories, confirmed a significantly elevated expression of the Qk gene in the aged group ($P<0.05$)(data not shown). Since Qk was also located in the "vasculature" related categories and furthermore has a function in embryonic vasculogenesis [21], we performed additional experiments to gain insight in Qk expression and cellular function in regard to aging and atherosclerosis.

Quaking expression increases with advancing age

To examine vascular Qk expression pattern in more detail, we performed an expression analysis on aortas harvested at increasing time points in ApoE-/- and WT mice, which had been fed a normal chow diet. This experiment confirmed the observation that Qk expression levels rise with advancing age. As depicted in figure 6A-B, no differences exist between 5 and 15 weeks of age. Strikingly, we observed a sharp 15-fold increase in Qk expression level in WT mice and a 7-fold increase in ApoE -/- mice from week 15 onwards which is in both cases highly significant after post hoc testing ($P<0.001$). These data are suggestive of an intrinsic role of Qk in age related vascular homeostasis per se rather than atherosclerosis, as the aortas of chow-fed aged ApoE-/- also contained some atherosclerotic plaque (data not shown), or, possibly, as vascular patency sensor. Since Qk protein expression has never been demonstrated in atherosclerotic

Figure 5.

Box	Ratio of enrichment	P-value	Box genes	Fold Change
1	7.8	0.0061	Nr2f2 Hey2 Quaking	2.13 1.52 1.74
2	8.1	0.0058	Nr2f2 Hey2 Quaking	2.13 1.52 1.74
3	9.4	0.0038	Nr2f2 Hey2 Quaking	2.13 1.52 1.34
4	50	0.0007	Hey2 Quaking	1.52 1.74
5	1.3	0.0024	28 genes	
6	14.3	0.0083	Lcn5 Tpk1	-1.83 -1.65
7	13.3	0.0097	Usp33 Usp4	1.42 -1.32
8	18.2	0.0051	Lcn5 Gnpda2	-1.83 1.59

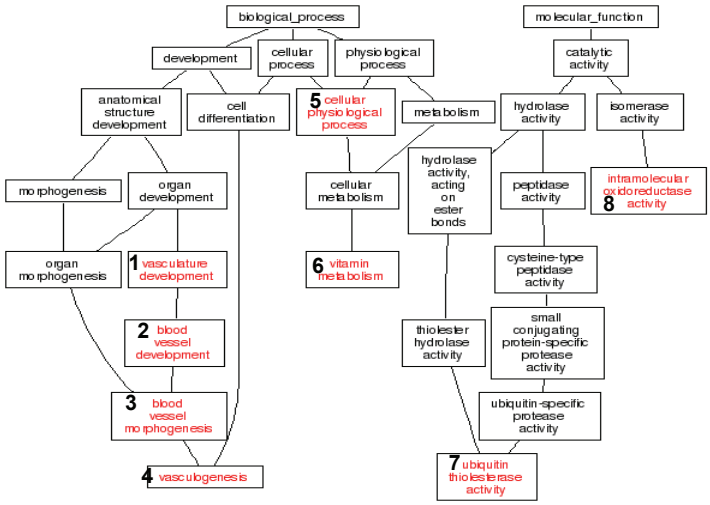

Gene Ontology (GO) pathways, categorized in biological process and molecular function. Significant altered gene categories, containing both up- and/or down-regulated genes, between aged and young mice are highlighted in red. Ratio of enrichment = the number of observed genes/ the number of expected genes. For color figure see page: 226

plaques, we have assessed the expression pattern of Qk protein in carotid artery and aortic root sections of young and aged LDLr-/- mice. We did not only observe a surprisingly clear Qk protein expression in endothelial cells, macrophages and vascular smooth cells in carotid and aortic root plaques, we also noticed Qk expression in endothelial cells of plaque-free coronary

Figure 6.

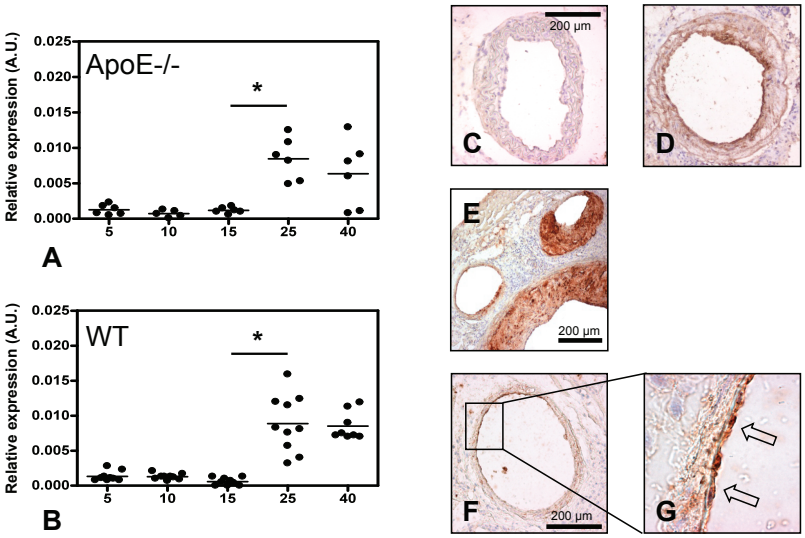

Qk expression is present in the vasculature, both dependent and independent of atherosclerosis. Qk gene expression in the aortic arch dramatically increases between 15 and 25 weeks of age in ApoE-/- and wild-type mice (devoid of atherosclerotic plaque) fed a chow diet (A,B). Qk protein expression is detected in mouse carotid arteries. Staining with reference isotype IgG shows no staining, whereas atherosclerotic plaques show abundant staining for Qk protein (C,D). Qk staining is also observed in aortic root sections, mainly within the atherosclerotic plaque (E). Staining mouse coronary arteries devoid of plaque, Qk expression is clearly seen in endothelial cells (arrowheads) (F,G). * $P<0.001$, A.U. = arbitrary units. For color figure see page: 227

Figure 7.

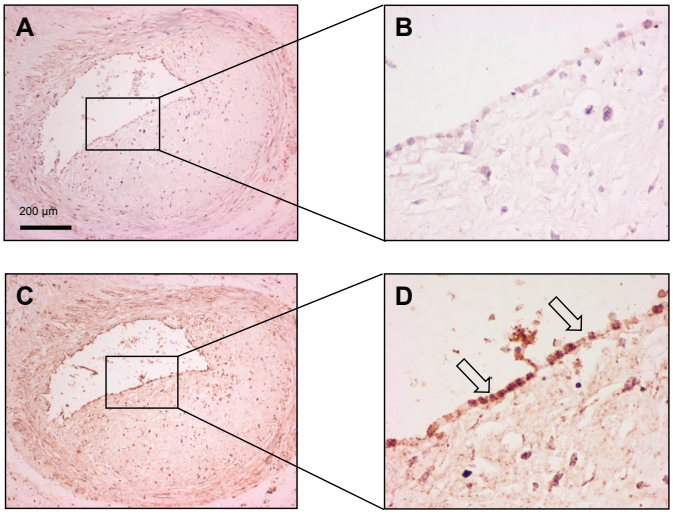

Quaking expression is detected in human coronary arteries. Staining with reference isotype IgG reveals no staining (A,B). Quaking protein expression is detected in human atherosclerotic plaques and is mainly located in the endothelium (C,D). For color figure see page: 227

arteries as well (figure 6C-G). However, it was not possible to perform a quantitative analysis of Qk expression between groups. Not only did we observe Qk staining in mouse sections, human atherosclerotic plaques also showed Qk protein expression which was again mainly located in endothelial cells (figure 7A-D).

DISCUSSION

In the present study, aging was accompanied by an impaired capacity to adapt to changes in diet cholesterol loads, and by a decreased atherogenenic and outward remodeling response in LDLr-/- mice. Aging furthermore induced differential expression of 41 genes in the carotid artery, of which Qk seems a prominent new atherosclerotic target gene.

Contrary to our initial expectations, we detected an increased atherogenic response at two vascular beds in young LDLr-/- mice compared to aged mice after feeding a high fat diet for an identical period of time. This observation is in concordance with Cortes et al., who observed that 4 to 5 year old rabbits had markedly reduced atherosclerotic lesion formation compared with 5 months old counterparts, despite the same dietary regimen [12]. However Merat et al., focussing on early lesion formation, reported feeding young and aged LDLr-/- mice with high fat diet aggravated the atherogenic response in aged mice at the aortic root, which is in contrast with our results [4]. Although not a very extensively studied topic, processing capacity of cholesterol was shown to be impaired in aged animals in at least two studies, leading to increased serum cholesterol levels and excessive accumulation of fat in various organs like the liver, adipose tissue and blood vessels [22, 23]. Very little is known about the age related adaptive response of cholesterol homeostasis in response to high fat diet feeding. Our data are suggestive for an enhanced capacity to adapt to changed fat and cholesterol intake as serum cholesterol levels in aged mice adjusted to new equilibrium levels more gradually after starting high fat diet feeding as compared to young mice. As serum cholesterol levels and the atherosclerotic burden did not correlate in our study, neither at the carotid artery nor at the aortic root level, the observed differences in plaque area are probably only partly caused by differential cholesterol levels. Altogether, we may firmly conclude that vascular aging is not associated with an increased atherogenic response.

Intriguingly, the reduced atherogenic propensity of aged LDLr-/- mice was accompanied by reduced compensatory outward remodeling of the carotid artery. Arterial outward remodeling is an important vascular adaptive process upon atherogenesis in order to maintain sufficient blood flow to the downstream organs [24]. In human coronary arteries, the outward remodeling response is gradually attenuated with advancing age, which may be partly ascribed to age induced endothelial dysfunction [25, 26]. As we did not observe any differences in TVA at a non-atherosclerotic segment of the carotid tree and given that LDLr-/- mice do not develop atherosclerosis on a chow diet, the difference in TVA between young and aged mice is solely caused by a differential response of the vessel wall to atherosclerosis. This is underscored by the

significant correlation between plaque area and TVA in young mice, whereas in aged mice such a correlation was absent. Next to endothelial dysfunction, this difference might be ascribed to the increased vascular stiffening seen in aging [11], rendering the arteries more rigid and reducing their adaptive outward remodeling capacity.

In contrast to our expectations we did not observe major differences in surrogate parameters of plaque stability in the carotid artery. Although not significant, VSMC content as indicated by α-actin staining in plaques of aged mice tended to be increased, pointing to more extensive VSMC infiltration into the atherosclerotic plaque. This is in concordance with the enhanced fibroproliferative response to vascular injury seen in aged mice [27]. Overall the plaque phenotype in aged and young mice was essentially similar.

To pinpoint the pathways underlying the reduced adaptive remodeling capacity in aged mice we have compared the gene expression profiles of atherosclerotic vessel segments from aged versus young mice. Tabibiazar et al. have previously examined age-related differences in vascular gene expression between two mouse strains but did not include an intra-strain analysis [28]. It should be emphasized that while the substrate of analysis is rather heterogeneous tissue comprising various cell types, the plaque composition in young and aged mice was rather equal, excluding that compositional differences may have biased our analysis. However, we cannot exclude that the difference in plaque size biased our analysis. After adjustment for multiple testing, relatively few genes (41 in total) were differentially regulated between aged and young mice. Of the genes that were up-regulated in the vasculature upon aging, Quaking (Qk) and Abl-interactor-2 were seen to play a role in age-dependent embryonic development of the central nervous system [29, 30]. Of the down-regulated genes, decreased expression of the antioxidant enzyme Catalase has been associated with aging and was seen to decrease with age in aortic walls of ApoE-/- mice [31, 32]. Age dependent regulation of the remaining genes has thus far not been documented. Subsequent Gene Ontology (GO) categorisation showed differentially regulated categories in the "biological process" and "molecular function" sectors of the GO tree. Significant differentially regulated categories contained at least two significantly regulated genes. As the "cellular physiological process" category is a broad up-stream component of this analysis it contained a wide amount of regulated genes, however with relatively low ratio of enrichment. The "vasculature development" gene set and 3 downstream categories were all significantly regulated and may thereby form an interesting pathway in the context of vascular aging. These categories contained the 3 up-regulated genes Nr2f2, Hey2 and Qk, all of which were seen to be implicated in vascular development and remodeling. Nr2f2 is involved in angiogenic and vascular remodeling processes in developing murine embryos, and Nr2f2 mutant mice die in utero [33]. Also, knockout Hey2 mice not only showed reduced neo-intima formation and proliferation after arterial wire injury, but also decreased proliferation in cultured VSMCs derived from these mice [34]. Transcript levels of Nr2f2 and Hey2 may therefore be increased in response to a decreased remodeling capacity in aged mice.

This may also account for Qk, as it might be a particularly interesting gene in the context of remodeling. Qk is a RNA-binding protein and a member of the signal transduction and

activation of RNA (STAR) family and been identified as key regulator in central nervous system development [35], and is involved in vascular development in utero by regulating factors implicated in vascular remodeling [21]. We now extend these embryonic observations by showing that Qk expression is induced during age related vascular homeostasis. Since the temporal expression pattern in control and atherosclerotic arteries were identical, the age dependent up-regulation of Qk is an intrinsic feature of the artery. Further studies are required to establish the significance of Qk up-regulation for (age related) vascular remodeling responses.

In conclusion, aging is accompanied by an impaired atherogenic and vascular remodeling response in LDLr-/- mice without being accompanied by major differences in plaque morphology. Gene profiling revealed a relatively small number of genes regulated upon vascular aging, of which genes regulating embryonic vasculature development may be the most relevant. We have identified the transcriptional regulator Quaking as an intriguing new player in adult vascular homeostasis and its function during aging deserves to be explored in future research.

REFERENCES

1. Strong JP, McGill HC, Jr. The Natural History of Aortic Atherosclerosis: Relationship to Race, Sex, and Coronary Lesions in New Orleans. *Exp Mol Pathol.* 1963;52:SUPPL1:15-27.
2. Orlandi A, Bochaton-Piallat ML, Gabbiani G, Spagnoli LG. Aging, smooth muscle cells and vascular pathobiology: implications for atherosclerosis. *Atherosclerosis.* 2006;188:221-230.
3. Lakatta EG. Arterial and cardiac aging: major shareholders in cardiovascular disease enterprises: Part III: cellular and molecular clues to heart and arterial aging. *Circulation.* 2003;107:490-497.
4. Merat S, Fruebis J, Sutphin M, Silvestre M, Reaven PD. Effect of aging on aortic expression of the vascular cell adhesion molecule-1 and atherosclerosis in murine models of atherosclerosis. *J Gerontol A Biol Sci Med Sci.* 2000;55:B85-94.
5. Egashira K, Inou T, Hirooka Y, Kai H, Sugimachi M, Suzuki S, Kuga T, Urabe Y, Takeshita A. Effects of age on endothelium-dependent vasodilation of resistance coronary artery by acetylcholine in humans. *Circulation.* 1993;88:77-81.
6. Lakatta EG, Levy D. Arterial and cardiac aging: major shareholders in cardiovascular disease enterprises: Part I: aging arteries: a "set up" for vascular disease. *Circulation.* 2003;107:139-146.
7. McCaffrey T, Nicholson A, Szabo P, Weksler M, Weksler B. Aging and arteriosclerosis. The increased proliferation of arterial smooth muscle cells isolated from old rats is associated with increased platelet-derived growth factor-like activity. *J. Exp. Med.* 1988;167:163-174.
8. Li Z, Cheng H, Lederer WJ, Froehlich J, Lakatta EG. Enhanced Proliferation and Migration and Altered Cytoskeletal Proteins in Early Passage Smooth Muscle Cells from Young and Old Rat Aortic Explants. *Experimental and Molecular Pathology.* 1997;64:1-11.
9. Ruiz-Torres A, Gimeno A, Melon J, Mendez L, Munoz FJ, Macia M. Age-related loss of proliferative activity of human vascular smooth muscle cells in culture. *Mech Ageing Dev.* 1999;110:49-55.
10. Vigetti D, Moretto P, Viola M, Genasetti A, Rizzi M, Karousou E, Pallotti F, De Luca G, Passi A. Matrix metalloproteinase 2 and tissue inhibitors of metalloproteinases regulate human aortic smooth muscle cell migration during in vitro aging. *Faseb J.* 2006;20:1118-1130.
11. Zieman SJ, Melenovsky V, Kass DA. Mechanisms, pathophysiology, and therapy of arterial stiffness. *Arterioscler Thromb Vasc Biol.* 2005;25:932-943.
12. Cortes MJ, Diez-Juan A, Perez P, Perez-Roger I, Arroyo-Pellicer R, Andres V. Increased early atherogenesis in young versus old hypercholesterolemic rabbits by a mechanism independent of arterial cell proliferation. *FEBS Lett.* 2002;522:99-103.
13. Orlandi A, Marcellini M, Spagnoli LG. Aging influences development and progression of early aortic atherosclerotic lesions in cholesterol-fed rabbits. *Arterioscler Thromb Vasc Biol.* 2000;20:1123-1136.
14. von der Thusen JH, van Berkel TJ, Biessen EA. Induction of rapid atherogenesis by perivascular carotid collar placement in apolipoprotein E-deficient and low-density lipoprotein receptor-deficient mice. *Circulation.* 2001;103:1164-1170.
15. Reljic R, Ries M, Anic N, Ries B. New chromogen for assay of glucose in serum. *Clin Chem.* 1992;38:522-525.
16. Bligh EG, Dyer WJ. A rapid method of total lipid extraction and purification. *Can J Biochem Physiol.* 1959;37:911-917.
17. Van Gelder RN, von Zastrow ME, Yool A, Dement WC, Barchas JD, Eberwine JH. Amplified RNA synthesized from limited quantities of heterogeneous cDNA. *Proc Natl Acad Sci U S A.* 1990;87:1663-1667.
18. Benjamini Y, Hochberg Y. Controlling the false discovery rate: a practical and powerful approach to multiple testing. *J. Roy. Stat. Soc. B.* 1995;57:289-300.
19. Zhang B, Schmoyer D, Kirov S, Snoddy J. GOTree Machine (GOTM): a web-based platform for interpreting sets of interesting genes using Gene Ontology hierarchies. *BMC Bioinformatics.* 2004;5:16.
20. Schoneveld A, Hoefer I, Sluijter J, Laman J, De Kleijn D, Pasterkamp G. Atherosclerotic lesion development and Toll like receptor 2 and 4 responsiveness. *Atherosclerosis.* 2007.
21. Noveroske JK, Lai L, Gaussin V, Northrop JL, Nakamura H, Hirschi KK, Justice MJ. Quaking is essential for blood vessel development. *Genesis.* 2002;32:218-230.
22. Takeuchi N, Ito M, Yamamura Y. Cholestero metabolism in rats sensitive to high cholesterol diet. *Adv Exp Med Biol.* 1976;67:267-288.
23. Araki S, Okazaki M, Goto S. Impaired lipid metabolism in aged mice as revealed by fasting-induced expression of apolipoprotein mRNAs in the liver and changes in serum lipids. *Gerontology.* 2004;50:206-215.
24. Glagov S, Weisenberg E, Zarins CK, Stankunavicius R, Kolettis GJ. Compensatory enlargement of human atherosclerotic coronary arteries. *N Engl J Med.* 1987;316:1371-1375.
25. Ishida S, Hamasaki S, Kamekou M, Yoshitama T, Nakano F, Yoshikawa A, Kataoka T, Saihara K, Minagoe S, Tei C. Advancing age is associated with diminished vascular remodeling and impaired vasodilation in resistance coronary arteries. *Coron Artery Dis.* 2003;14:443-449.
26. Brandes RP, Fleming I, Busse R. Endothelial aging. *Cardiovasc Res.* 2005;66:286-294.
27. Vazquez-Padron RI, Lasko D, Li S, Louis L, Pestana IA, Pang M, Liotta C, Fornoni A, Aitouche A, Pham SM. Aging exacerbates neointimal formation, and increases proliferation and reduces susceptibility to apoptosis of vascular smooth muscle cells in mice. *J Vasc Surg.* 2004;40:1199-1207.

28. Tabibiazar R, Wagner RA, Spin JM, Ashley EA, Narasimhan B, Rubin EM, Efron B, Tsao PS, Tibshirani R, Quertermous T. Mouse Strain-Specific Differences in Vascular Wall Gene Expression and Their Relationship to Vascular Disease. *Arterioscler Thromb Vasc Biol.* 2004.
29. Courtney KD, Grove M, Vandongen H, Vandongen A, LaMantia AS, Pendergast AM. Localization and phosphorylation of Abl-interactor proteins, Abi-1 and Abi-2, in the developing nervous system. *Mol Cell Neurosci.* 2000;16:244-257.
30. Hardy RJ, Loushin CL, Friedrich VL, Jr., Chen Q, Ebersole TA, Lazzarini RA, Artzt K. Neural cell type-specific expression of QKI proteins is altered in quakingviable mutant mice. *J Neurosci.* 1996;16:7941-7949.
31. Schriner SE, Linford NJ, Martin GM, Treuting P, Ogburn CE, Emond M, Coskun PE, Ladiges W, Wolf N, Van Remmen H, Wallace DC, Rabinovitch PS. Extension of murine life span by overexpression of catalase targeted to mitochondria. *Science.* 2005;308:1909-1911.
32. t Hoen PA, Van der Lans CA, Van Eck M, Bijsterbosch MK, Van Berkel TJ, Twisk J. Aorta of ApoE-deficient mice responds to atherogenic stimuli by a prelesional increase and subsequent decrease in the expression of antioxidant enzymes. *Circ Res.* 2003;93:262-269.
33. Pereira FA, Qiu Y, Zhou G, Tsai MJ, Tsai SY. The orphan nuclear receptor COUP-TFII is required for angiogenesis and heart development. *Genes Dev.* 1999;13:1037-1049.
34. Sakata Y, Xiang F, Chen Z, Kiriyama Y, Kamei CN, Simon DI, Chin MT. Transcription factor CHF1/Hey2 regulates neointimal formation in vivo and vascular smooth muscle proliferation and migration in vitro. *Arterioscler Thromb Vasc Biol.* 2004;24:2069-2074.
35. Vernet C, Artzt K. STAR, a gene family involved in signal transduction and activation of RNA. *Trends Genet.* 1997;13:479-484.